

A Density Functional Study of the Systems  $[\text{MH}_3(\text{PMe}_3)_4]^+$  ( $\text{M} = \text{Fe}, \text{Ru}, \text{Os}$ )

Heiko Jacobsen and Heinz Berke\*

Anorganisch-Chemisches Institut der Universität Zürich,  
Winterthurerstrasse 190, CH-8057 Zürich, Switzerland  
Fax: (internat.) +41(0)1/364-0191  
E-mail: hberke@aci.unizh.ch

Received May 6, 1997

**Keywords:** Transition metal / Complexes of the iron triad / Density functional calculations / Relativistic effects / Hydrido complexes

The structures and relative energies of various isomers of  $[\text{FeH}_3(\text{PMe}_3)_4]^+$  (**1**),  $[\text{RuH}_3(\text{PMe}_3)_4]^+$  (**2**) and  $[\text{OsH}_3(\text{PMe}_3)_4]^+$  (**3**) have been studied by density functional theory. The stereoisomers considered are derived from a tetrahedral (T), square planar (P), and  $\text{C}_{2v}$ -butterfly (C) arrangement of the phosphane ligands. For the latter two, classical trihydride (I) and nonclassical hydride/dihydrogen (II) geometries have

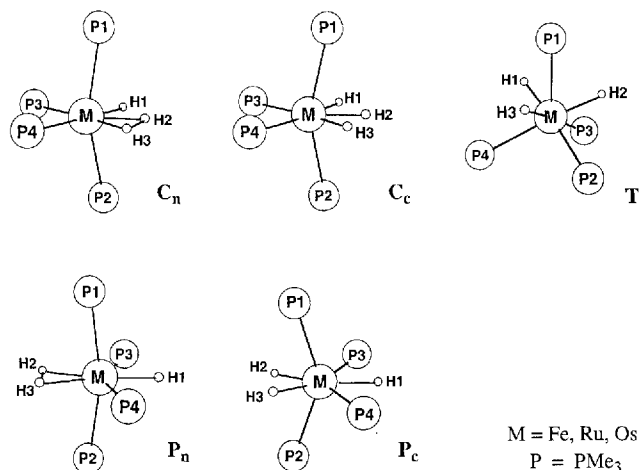
been considered. **1** and **2** prefer coordination mode II, whereas **3** favors coordination mode I. This trend is explained by relativistic effects. For Fe and Os, the C and T type structures are preferred over a P geometry. For Ru, the C and P structures are close in energy, and the T arrangement represents the highest energy isomer.

## Introduction

Many transition metal hydride complexes are stereochemically nonrigid in solution.<sup>[1]</sup> Different isomers coexist, and the dynamic behavior as well as the hydride fluxionality are characteristic features for these systems. One class of transition metal hydride complexes that is of particular interest, are the cationic complexes of the iron triad  $[\text{MH}_3\text{L}_4]^+$  ( $\text{M} = \text{Fe}, \text{Ru}, \text{Os}$ ), where L represents mono- to tetradentate phosphorus ligands.<sup>[2]</sup> The possible coordination geometries of these molecules can be classified as *P*-, *C*-, and *T*-type structures. Here, the *P*, *C*, and *T* nomenclature is derived from the coordination sphere of the ligands L, based on a square planar,  $\text{C}_{2v}$ -butterfly or tetrahedral arrangement. Further, one has to differentiate between classical trihydride complexes, and nonclassical hydride–dihydrogen systems, in which one  $\text{H}_2$  ligand is bonded to the metal center through both hydrogens. We designate these types as  $\text{C}_c$  and  $\text{C}_n$ , or  $\text{P}_c$  and  $\text{P}_n$ , respectively. Figure 1 shows representative examples for the various coordination modes.

In our group, we recently characterized the structures and dynamics of cationic group VIII complexes with monodentate trialkylphosphane ligands  $[\text{MH}_3(\text{PR}_3)_4]^+$  ( $\text{M} = \text{Fe}, \text{Ru}, \text{Os}$ ;  $\text{R} = \text{Me}, \text{Et}$ ).<sup>[3]</sup> For the systems containing the  $\text{PMe}_3$  ligand, it was found that in solution the iron and osmium species form equilibrium mixtures between the *C*- and the *T*-type isomers, whereas the ruthenium compound solely exists as *C*-type structure. For the *C*-isomers, one observes nonclassical hydride coordination only for iron and ruthenium, whereas the osmium complex prefers the classical trihydride coordination. We also initiated a companion theoretical study,<sup>[4]</sup> based on density functional theory (DFT),<sup>[5]</sup> in which we investigated different isomers of

Figure 1.  $\text{C}_n$ ,  $\text{C}_c$ ,  $\text{P}_n$ ,  $\text{P}_c$  and *T* geometries of  $[\text{M}(\text{PMe}_3)_4\text{H}_3]^+$  ( $\text{M} = \text{Fe}, \text{Ru}, \text{Os}$ )



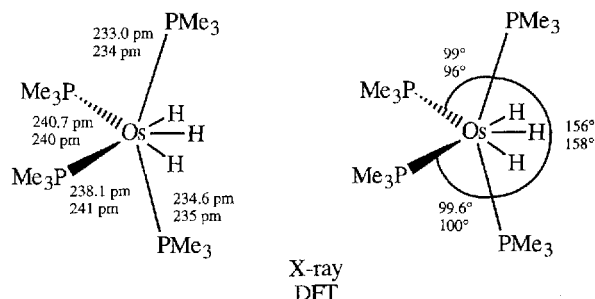
$[\text{FeH}_3(\text{PR}_3)_4]^+$  ( $\text{R} = \text{H}, \text{CH}_3$ ). One of our findings was that the trimethylphosphane ligand cannot successfully be modelled by  $\text{PH}_3$ . The different donor properties of  $\text{PH}_3$  and  $\text{PMe}_3$  lead to a different energy ranking of the isomers of  $[\text{FeH}_3(\text{PH}_3)_4]^+$  and  $[\text{FeH}_3(\text{PMe}_3)_4]^+$ . In connection with this problem, we also discussed possible mechanisms for the hydrogen exchange of the latter species.

In the present paper, we extend our theoretical studies to include complexes of the two heavier members of the iron triad. Our work centers around the structures and relative energies of various isomers of  $[\text{FeH}_3(\text{PMe}_3)_4]^+$  (**1**),  $[\text{RuH}_3(\text{PMe}_3)_4]^+$  (**2**) and  $[\text{OsH}_3(\text{PMe}_3)_4]^+$  (**3**). The iron isomers are included in this work, in order to be able to study group trends.

## Results and Discussion

We optimized the geometries of the  $C_n$ ,  $C_c$ ,  $P_n$ ,  $P_c$  and  $T$  isomers of **1**, **2**, and **3**. Selected structural parameters are collected in Table 1. For two of the compounds, namely  $C_n$ -**1** and  $C_c$ -**3**, there exist structural data obtained from X-ray diffraction studies.<sup>[3]</sup> The crystal structure of a related compound,  $T$ -[FeH<sub>3</sub>(PEt<sub>3</sub>)<sub>4</sub>]<sup>+</sup> (**4**), is also known.<sup>[3]</sup> The comparison between calculated structures and experimental data allows a first judgement of the quality of the method of calculation employed. The iron complexes have already been discussed in detail,<sup>[4]</sup> and here we briefly comment on the osmium system. The X-ray and DFT geometries for  $C_c$ -**3** are displayed in Scheme 1.

Scheme 1



The calculation reproduces the experimental structure reasonably well, with deviation of 1–3 pm in the Fe–P bond lengths, and 1°–3° in P–Fe–P bond angles. Unfortunately, no direct comparison for the hydride ligands is possible. Their position in the X-ray structure does not provide reliable structural information, due to high standard deviations.<sup>[3]</sup>

We now discuss general trends observed for the different isomers. For all  $C_n$  structures, we note that the  $\text{PMe}_3$  ligand in *trans* position to the hydride forms the longest M–P bond (ligands P4 and H1 in Figure 1 and Table 1). For all  $T$  isomers, the phosphane ligand with no hydride in *trans* position shows a significantly shorter Fe–P separation, compared to the other phosphanes (ligand P1 in Figure 1 and Table 1). The same structural motifs can be found in the crystal structure of  $C_n$ -**1**, and  $T$ -**4**. They demonstrate the destabilizing *trans* influence of the hydride ligand. This effect has been previously investigated by Lin and Hall in an extensive study on classical and nonclassical transition metal polyhydrides.<sup>[6]</sup> Burdett and Albright<sup>[7]</sup> provide a more general perturbational approach to the problem of *trans* influence, also in connection with the hydride ligand.

The average M–P bond distance amounts to 225 pm (**1**), 240 pm (**2**), and 237 pm (**3**). Thus, the M–P bond length increases as  $\text{Fe} < \text{Os} < \text{Ru}$ . This trend in M–L bond lengths, M being the transition metals of one particular triad, has been found previously, and is well understood in terms of relativity.<sup>[8]</sup> One relativistic effect, which becomes important for the osmium isomers, is the contraction of the core orbitals.<sup>[9][10]</sup> This leads to a reduction of the Pauli repulsion, which represents the destabilizing two-orbital four-electron interactions between the metal center and the

ligand. This is the main cause for the relativistic bond contraction, as found for the osmium systems.

The average M–H<sub>H</sub> bond length, H<sub>H</sub> being a hydride ligand, amounts to 151 pm (**1**), 165 pm (**2**), and 167 pm (**3**). Since the hydride ligand does not possess any core orbitals, the reduced Pauli repulsion is of only minor importance, and one observes the following trend for the M–H separation:  $\text{Fe} < \text{Ru} < \text{Os}$ . This tendency correlates with the increasingly diffuse character of the valence d orbitals, when going down the triad.

The average M–H<sub>H<sub>2</sub></sub> bond length, H<sub>H<sub>2</sub></sub> belonging to a dihydrogen ligand, amounts to 159 pm (**1**), 178 pm (**2**), and 173 pm (**3**). Here, a second relativistic effect comes into play. The relativistic core contraction leads to a more effective shielding of the nucleus, and thus reduces the effective nuclear charge. As a result, the valence d-orbitals are destabilized, and raise in energy. Li and Ziegler have analyzed the consequences for the bonding of transition metal dihydrogen complexes.<sup>[11]</sup> To understand this effect, we have to briefly comment on the bonding of side-on coordinated dihydrogen to transition metal centers.<sup>[12]</sup> The primary interaction is believed to be donation from the dihydrogen  $\sigma$ -orbital to an empty  $d_{\sigma}$  orbital on the metal center, augmented by a weaker back donation of metal  $d_{\pi}$  electrons to the dihydrogen  $\sigma^*$  orbital. For osmium, both d orbitals are raised in energy, due to relativistic effects. The energy increase for  $d_{\pi}$  will enhance the back donation since this orbital is now closer in energy to the H<sub>2</sub>  $\sigma^*$  orbital. On the other hand, the energy increase for  $d_{\sigma}$  will reduce donation since the gap to the  $\sigma$  orbital on H<sub>2</sub> is enlarged. The interacting orbitals and their relative energies for the relativistic (r) and non-relativistic (nr) case are displayed in Scheme 2.<sup>[13]</sup>

The gain in back donation outweighs the loss in donation, so that on going from the ruthenium to the osmium isomers, the M–H<sub>H<sub>2</sub></sub> bond strengthens and gets shorter. This leads to the following trend in the M–H<sub>H<sub>2</sub></sub> distances:  $\text{Fe} < \text{Os} < \text{Ru}$ . Also, dihydrogen ligands coordinated to osmium show the longest H–H separation, compared to their analogues bonded to iron or ruthenium centers [distance  $d(\text{H}_2-\text{H}_3)$  in Table 1], indicating the largest amount of back donation. The same trend is experimentally found for the series of the related compounds  $[\text{M}(\text{depe})_2\text{H}_3]^+$  (M = Fe, Ru, Os;  $\text{depe} = \text{Et}_2\text{PCH}_2\text{CH}_2\text{PEt}_2$ ), which all adapt a  $P_n$ -type geometry.<sup>[14]</sup> The H–H distance of the  $\eta^2$ -bonded dihydrogen ligand could be determined by solution NMR methods. Under the assumption that the H<sub>2</sub> ligand is rapidly spinning, the H–H distances are 91 pm, 89 pm, and  $112 \pm 3$  pm for the iron, ruthenium, and osmium complex, respectively. Again, the largest value for  $d_{\text{H}-\text{H}}$  is observed for the osmium system.

The electron transfer from the metal center to the H<sub>2</sub> ligand further influences the valence tautomerism between nonclassical dihydrogen and classical dihydride coordination. The back donation might induce a complete cleavage of the H–H bond, if the electron transfer is too large. The relative energies of the isomers of **1**, **2**, and **3** are dis-

Table 1. Optimized bond distances<sup>[a]</sup> and bond angles<sup>[b]</sup> for the  $C_n$ ,  $C_c$ ,  $P_n$ ,  $P_c$  and  $T$  geometries of  $[M(PMe_3)_4H_3]^+$  ( $M = Fe, Ru, Os$ )<sup>[c]</sup>

	$C_n$			$C_c$			$P_n$			$P_c$			$T$		
	Fe	Ru	Os	Fe	Ru	Os	Fe	Ru	Os	Fe	Ru	Os	Fe	Ru	Os
d(M-H1)	152	165	167	151	165	166	152	164	168	153	169	170	152	165	168
d(M-H2)	156	174	168	149	160	164	160	180	176	150	165	166	152	165	168
d(M-H3)	160	178	170	152	165	166	161	181	176	151	165	167	152	164	167
d(M-P1)	225	240	237	227	240	234	226	240	238	226	239	238	215	228	228
d(M-P2)	226	239	236	225	239	235	227	241	236	224	240	234	226	242	240
d(M-P3)	225	236	237	228	247	240	224	239	234	222	240	236	226	243	240
d(M-P4)	228	247	243	228	245	241	224	240	239	225	240	241	226	242	240
d(H2-H3)	91	88	112	127	150	157	92	87	98	180	155	177	241	265	279
$\angle(H1-Fe-H2)$	68	73	69	57	55	62	163	166	164	141	152	147	107	113	101
$\angle(P1-Fe-P2)$	158	164	163	158	162	158	165	167	166	145	163	162	118	115	115
$\angle(P1-Fe-P3)$	93	98	100	100	100	96	92	92	92	98	93	93	119	124	125
$\angle(P1-Fe-P4)$	97	95	95	97	94	97	92	92	89	99	92	90	118	118	119
$\angle(P3-Fe-P4)$	102	99	94	98	97	95	145	154	155	123	141	139	99	98	97

[a] In pm. – [b] In degree. – [c] Compare Figure 1 for labelling of the ligands.

Scheme 2

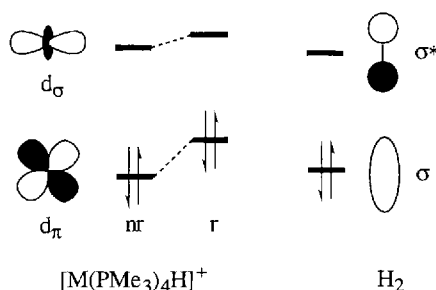
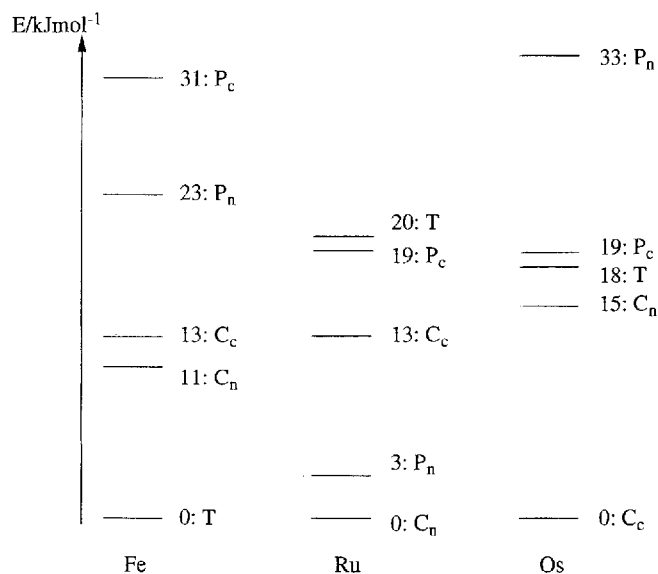


Figure 2. Relative energies of various isomers of  $[M(PMe_3)_4H_3]^+$  ( $M = Fe, Ru, Os$ ). For each metal, the lowest energy structure is set to zero



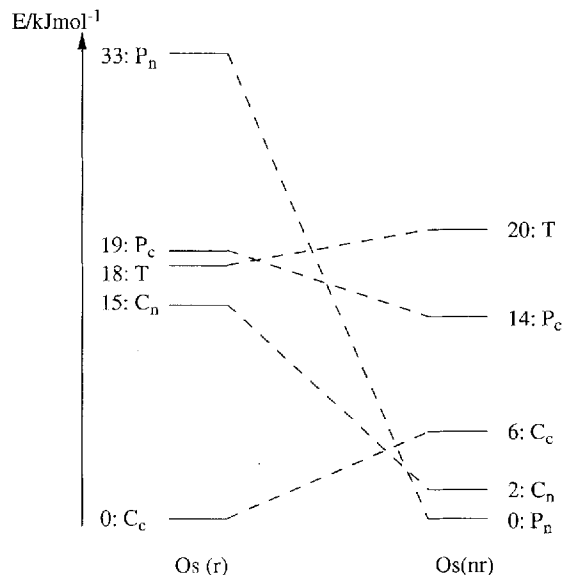
played in Figure 2. For each metal, the lowest energy structure is set to zero.

The coordination of the H ligands can be described either as *cis* H<sub>2</sub>(2H) structure, as in the *C*-type isomers, or as *trans* H<sub>2</sub>(2H) structure, as in the *P*-type isomers. Here, (2H) stands for either the dihydrogen ligand, or two hydride ligands. For all systems, we find that the *cis* structure is energetically favored over the *trans* arrangement. This is in agreement with the experiment; *trans* structures have not been observed for any of the systems under investigation.<sup>[3]</sup> However, one has to keep in mind that not only thermodynamics, but also kinetics have to be considered. The *P*-type structures may not be accessible due to a high activation barrier of the isomerisation process. More detailed mechanistic studies are necessary in order to investigate the dynamics of  $[MH_3(PMe_3)_4]^+$  systems. Also in accordance with the experimental findings is the fact that iron and ruthenium complexes favor the nonclassical *C* and *P* structures, whereas osmium shows a preference for the classical coordination. As mentioned above, the enhanced back donation from the metal center to the H<sub>2</sub> ligand causes breaking of the H–H bond, and leads to the classical trihydride complex. For iron and osmium, the *P*-type structures are the least stable arrangements, and one finds the following energy ranking: for Fe ( $T < C_n < C_c$ ) < ( $P_n < P_c$ ) and for Os ( $C_c < C_n < T$ ) < ( $P_c < P_n$ ). On the other hand, for ruthenium, we find the *T* structure as the highest energy isomer, and obtain the following ranking: ( $C_n < P_n$ ) < ( $C_c < P_c$ ) < *T*.

We have seen that relativistic effects are of special importance for the osmium system **3**. To further illustrate this point, we performed single point calculations without explicit treatment of relativistic effects for the five isomers of **3**. The results are presented in Figure 3. We now find indeed the nonclassical structures at lower energies than the classi-

cal ones. Most remarkable is the destabilisation of the  $P_n$ -isomer by relativistic effects: For **3(nr)**,  $P_n$  represents to be the most stable, for **3(r)**, the least stable isomer.

Figure 3. Influence of relativistic effects on the relative energies of the various isomers of  $[\text{Os}(\text{PMe}_3)_4\text{H}_3]^+$  (r) and (nr) refer to relativistic and non relativistic calculations, respectively



The energy scale for the isomers of **3(nr)** is very similar to that of **2**. The most stable isomers are in both cases the  $C_n$  and the  $P_n$  structures. Ruthenium slightly favors the *cis* structure by 3 kJ/mol, whereas osmium shows a preference for the *trans* arrangement by only 2 kJ/mol. For both structures, the *T* isomer is least favorable on energetic grounds. Without consideration of relativistic effects, one would find the following group trends:  $P_c$ -isomers are stabilized, and *T* isomers are destabilized when going down the triad. It is the influence of relativity which makes the osmium system more comparable to its iron rather than to its ruthenium counterpart.

For the *T* isomers, one observes a dynamic behaviour of hydride reorientation in solution.<sup>[3]</sup> The rate for this fluxional process varies with the transition metal involved. For the iron complex, the barrier for the rearrangement process could be estimated to roughly amount to 33 kJ/mol. The osmium complex shows a faster rate of exchange, and the barrier must be lower than 27 kJ/mol. We proposed that the  $P_c$  structure could play a role as an intermediate close to the transition state, or as a possible transition state in the hydrogen exchange reaction.<sup>[4]</sup> Our calculated energy difference between *T*-1 and  $P_c$ -1 of 31 kJ/mol corresponds well with the experimentally obtained value.<sup>[3]</sup> The very small energy difference between *T*-3 and  $P_c$ -3 supports the notion of a very fast hydrogen exchange in the osmium complex.

## Conclusion

We will summarize our present study in a few final remarks. We have investigated the structures and relative ener-

gies of various isomers of  $[\text{MH}_3\text{L}_4]^+$  ( $\text{M} = \text{Fe}, \text{Ru}, \text{Os}$ ). One main aspect of our work is the relative stability of classical and nonclassical isomers. In accordance with experimental observations, we found that the iron and ruthenium complexes prefer a nonclassical  $C_n$  and  $P_n$  coordination over  $C_c$  and  $P_c$  geometries. For the osmium system, relativistic effects become of special importance. The effects of relativistic core contraction and destabilisation of valence d orbitals lead to a preference for classical trihydride coordination. Of further importance is the relative stability of the *P*, *C* and *T*-type structures. Without relativity, the *P* structures would be stabilized, and the *T* geometries would be destabilized, when going down the triad. It is again the influence of relativistic effects which makes the osmium complex more comparable to its iron rather than to its ruthenium counterpart.

This work was supported by the Swiss National Science Foundation (SNSF). Access to the computing facilities of the Rechenzentrum der Universität Zürich is gratefully acknowledged.

## Computational Details

**Computational Details:** All calculations are based on the local density approximation (LDA) in the parametrization of Vosko, Wilk and Nussair,<sup>[15]</sup> with the addition of gradient corrections due to Becke<sup>[14]</sup> and Perdew<sup>[16]</sup> (GGA). The GGA was included self-consistently (NL-SCF). The calculations utilized the Amsterdam Density Functional package ADF,<sup>[17]</sup> release 2.0.1. Use was made of the frozen core approximation. For C and P, the valence shells were described using a double  $\zeta$ -STO basis, augmented by one *d*-STO polarization function (ADF database III). For the *n* s, *n* p, *n* d, (*n* + 1)s and (*n* + 1)p shells on the transition metals, a triple  $\zeta$ -STO basis was employed (ADF database IV with three (*n* + 1)p functions). H was treated with a double  $\zeta$ -STO basis and one additional *p*-STO polarization function (ADF database III). For the osmium isomers, relativistic effects were included using a quasi-relativistic approach,<sup>[18]</sup> if not mentioned otherwise. The numerical integration grid was chosen in a way that significant test integrals are evaluated with an accuracy of at least four significant digits. No symmetry constraints were applied in the calculations. All molecules have been fully optimized at the quantum mechanical level.

- [1] D. G. Gusev, H. Berke *Chem. Ber.* **1996**, *129*, 1143.
- [2] See ref. 3 for a compilation of known  $[\text{MH}_3(\text{PR}_3)_4]^+$  ( $\text{M} = \text{Fe}, \text{Ru}, \text{Os}$ ) complexes.
- [3] D. G. Gusev, R. Hübener, P. Burger, O. Orama, H. Berke, *J. Am. Chem. Soc.* **1997**, *119*, 3716.
- [4] H. Jacobsen, H. Berke *Chem. Eur. J.* **1997**, *3*, 881.
- [5] [5a] T. Ziegler, *Chem. Rev.* **1991**, *91*, 651. — [5b] T. Ziegler, *Can. J. Chem.* **1995**, *73*, 743.
- [6] Z. Lin, M. B. Hall, *J. Am. Chem. Soc.* **1992**, *114*, 6102.
- [7] J. K. Burdett, T. A. Albright, *Inorg. Chem.* **1979**, *18*, 2112.
- [8] [8a] J. Li, G. Schreckenbach, T. Ziegler, *J. Phys. Chem.* **1994**, *98*, 4838. — [8b] H. Jacobsen, G. Schreckenbach, T. Ziegler, *J. Phys. Chem.* **1994**, *98*, 11406.
- [9] [9a] P. Pykkö, J.-P. Declaux, *Acc. Chem. Res.* **1979**, *12*, 276. — [9b] P. Pykkö, *Chem. Rev.* **1988**, *88*, 563.
- [10] W. H. E. Schwarz, E. M. van Wezenbeck, E. J. Baerends, J. G. Snijders, *J. Phys. B* **1989**, *22*, 1515.
- [11] [11a] J. Li, R. M. Dickson, T. Ziegler, *J. Am. Chem. Soc.* **1995**, *117*, 11482. — [11b] J. Li, T. Ziegler, *Organometallics* **1996**, *15*, 3844.
- [12] [12a] J. Saillard, R. Hoffmann, *J. Am. Chem. Soc.* **1984**, *106*, 2006. — [12b] Y. Jean, A. Lledos, B. Maouche, R. Aïad, *J. Chim. Phys.* **1987**, *84*, 806.

- [13] Scheme 2 adopted from ref.<sup>[11a]</sup>.  
[14] M. T. Bautista, K. A. Earl, P. A. Maltby, R. H. Morris, C. T. Schweitzer, A. Sella, *J. Am. Chem. Soc.* **1988**, *110*, 7031.  
[15] S. J. Vosko, M. Wilk, M. Nussair, *Can. J. Phys.* **1980**, *58*, 1200.  
[16] A. Becke, *Phys. Rev.* **1988**, *A38*, 3098.  
[17] J. P. Perdew, *Phys. Rev.* **1986**, *B33*, 8822.  
[18] [18a] E. J. Baerends, D. E. Ellis, P. E. Ros, *Chem. Phys.* **1973**, *2*, 41. — [18b] G. teVelde, E. J. Baerends, *J. Comp. Phys.* **1992**, *99*, 84.  
[19] T. Ziegler, V. Tschinke, E. J. Baerends, J. G. Snijders, W. Ravenek, *J. Phys. Chem.* **1989**, *93*, 3050.

[97110]